International Journal of Research in Engineering and Science (IJRES)
ISSN (Online): 2320-9364, ISSN (Print): 2320-9356
www.ijres.org Volume 11 Issue 7 ǁ July 2023 ǁ PP. 114-119

Formation of biofilm on carriers in batch reactors as a method for reducing start-up time of UASB reactors

Christos A. Tzenos[1], Dimitra Pitsikoglou[1], Sotirios D. Kalamaras[1], George Em. Romanos[2], Themistoklis Sfetsas[3,*]

[1] *Department of Hydraulics, Soil Science and Agricultural Engineering, School of Agriculture, Aristotle University of Thessaloniki, GR-54124 Thessaloniki, Greece*

[2]*Institute of Nanoscience and Nanotechnology, National Center of Scientific Research "Demokritos", Agia Paraskevi, 15310 Athens, Greece;*

[*3]*QLAB Private Company, Research & Development, Quality Control and Testing Services, 57008 Thessaloniki, Greece;*

Corresponding Author: Themistoklis Sfetsas, t.sfetsas@q-lab.gr

Abstract

The aim of this paper is to create a method for reducing the start-up period of upflow anaerobic sludge blanket (UASB) reactors. For this purpose, anaerobic digestion experiments were performed in batch reactors containing two different biocarriers. Specifically, novel 3d-printed biocarriers made by 13X zeolite and bentonite (3DU) and commercial K1 rings (RU) were used for the creation of microbial biofilm on their surface. The batch reactors containing biocarriers showed improved performance compared to blank reactors, resulting in an increase in total methane production (mL CH_4 g^{-1} VS) of 14.01% and 16.04% for 3DU and RU, respectively. Biocarriers from the batch reactors were harvested and added to the UASB reactors to minimize their start-up period. Even though successful biogas production was observed in batch reactors with biocarriers, anaerobic digestion could not be sustained in UASB reactors after 2 attempts. The geometrical characteristics, pore size and type of material of the biocarriers was probably the reason for the UASB reactors failed operation.

Keywords: *UASB reactors, anaerobic digestion, biocarriers, methane production*

Date of Submission: 05-07-2023 Date of acceptance: 16-07-2023

I. INTRODUCTION

Biogas is produced via Anaerobic Digestion (AD), a biological process occurring in the absence of oxygen (O_2). The main constituents of biogas are methane (CH_4) and carbon dioxide (CO_2), with respective concentrations in the range of 50–70% and 30–50% [1]. A wide variety of organic wastes, including agricultural, municipal, and food industry waste, can be treated with AD, providing energy in the form of biogas, while simultaneously offering numerous environmental and economic benefits.

Upflow anaerobic sludge blanket (UASB) reactors produce biogas by AD while forming microbial aggregates. These aggregates are settled inside the reactor forming a blanket of granular sludge [2]. The operation of the UASB reactors is based on the creation and maintenance of the microbial aggregates that create a biofilm upon the surface of carriers, also referred as biocarriers, that are added inside the reactor. The main role of biocarriers is to provide a suitable surface for the microorganisms to attach to, enabling the formation of communities (biofilm) and protecting them from various stress factors [3]. They are made from a variety of materials, including aluminosilicates and polymers and come in many different shapes and sizes designed to increase their available surface. The physical parameters of the biocarriers, such as material, pore size and shape, influence the biofilm formation of microorganisms, as they allow or prevent access to available nutrients for their growth [4].

In the present study, novel biocarriers created by 3d-printing and synthesized by combining 13X zeolite and bentonite and commercially available K1 Ring (high density polyethylene, HDPE) were used as carriers for the creation of biofilm inside batch anaerobic reactors. The biocarriers with an anaerobic microflora attached were used for the operation of two lab-scale UASB reactors. The effect of the different biocarriers for reducing the startup time of the UASB reactors was investigated.

1.1 MATERIALS AND METHODS

1.1.1 3D-Printed Biocarriers

The novel 3D-printed biocarriers were created with a Bio X6 (Cellink, Gothenburg, Sweden) printer from Cellink, according to the methodology of Chioti, et al. [3]. A rectilinear geometric pattern was chosen, and the dimensions were 24 mm wide, 14 mm long, and 7 mm high with a repeating geometric pattern density of 18%. The base material of the biocarriers was, 13X zeolite (Alfa Aesar, Ward Hill, MA, United States) mixed with an inorganic composite material (bentonite) and an organic binder. A colloidal silicon/ionized aqueous solution was added to the solid mixture and was stirred until the viscous printing paste was produced. The solid content of the printing paste should exceed 50% to achieve the optimal density of the material.

1.1.2 Feedstock and inoculum

Inoculum from a full-scale mesophilic (37±1˚C) biogas plant in northern Greece was used in both batch and UASB reactors and to reduce its residual CH_4 production, it was pre-incubated for 7 days under anaerobic conditions at 37±0.5˚C. The synthetic substrate consisted of D-glucose ($C_6H_{12}O_6 \cdot H_2O$, Duchefa Biochemie, purity > 99.50%) as a carbon source and Basic Anaerobic Medium (BA Medium) as a nutrient source. The preparation of the BA medium was performed as described by Angelidaki and Sanders [5]. The characteristics of the inoculum are presented in Table 1.

Table 1. Inoculum characteristics

Parameter	Inoculum (Mean ± SD*)
Total Solids, TS (g L^{-1})	30.53 ± 2.74
Volatile Solids, VS (g L^{-1})	21.83 ± 1.73
Total Ammonia Nitrogen, TAN (mg N L^{-1})	1160 ± 12.76
Volatile Fatty Acids, VFA (g L^{-1})	1.58 ± 0.09
pH	7.75 ± 0.05

*SD, Standard Deviation.

1.1.3 Experimental setup

1.1.3.1 Anaerobic Biofilm Formation

Glass bottles were used as batch reactors with a total and working volume of 500 mL and 350 mL, respectively.3D printed biocarriers (no biofilm) were added to three batch reactors and that could displace 90 mL of water volume. The same procedure was done for the K1 ring commercial biocarriers. All the biocarriers were new and they weren't used before for biofilm formation. These 6 batch reactors with biocarriers were filled with 100 mL of inoculum and a solution of 1 g of D-glucose dissolved in 160 mL of deionized water to reach the working volume of 350mL. The volatile solids (VS) ratio of inoculum and glucose was approximately 1:2. Three reactors filled only with 100 mL of inoculum and a solution of 1 g of D-glucose dissolved in 250 mL and used as a blank. Also, three more reactors were used to measure methane production from inoculum. All the reactors were vigorously shaken by hand twice a day. Based on daily methane yield measurements, the beginning of the exponential phase was determined. On day 15, at the peak of the exponential phase, part of the biocarriers was harvested from the batch reactors and placed in the UASB reactors. All batch reactors were flushed with nitrogen gas (99.99% v v^{-1}) to ensure anaerobic conditions.

1.1.3.2 UASB Reactor Operation

Two UASB reactors with a total volume of 750 mL and an operating volume of 500 mL were used. The UASB reactors were equipped with an external water heating jacket, that maintained the internal temperature at 37±1˚C. The hydraulic retention time (HRT) was 4 days and the organic loading rate (OLR) of the synthetic substrate was 1 g VS d^{-1} L^{-1} for both reactors The biocarriers from the batch reactors were used to inoculate each UASB reactor covering 20% (100 mL) of the reactors' operating volume and the rest was filled with inoculum. In UASB1 and UASB2 the 3D-printed and K1 ring biocarriers were added, respectively. Prior to the start of the UASB reactors operation, nitrogen gas was used to establish anaerobic conditions.

1.1.4 Analytical Methods

Total solids (TS), VS, and total ammonia nitrogen (TAN) were determined following standard methods [6]. The pH value of the solutions was measured with a bench digital pH meter (JENWAY 3520, Essex, UK). The analysis of volatile fatty acids (VFA) samples was performed with a gas chromatograph (GC-2010plusAT, Shimadzu, Kyoto, Japan) equipped with a flame ionization detector (FID) with method parameters described previously in Kalamaras et al. [7]. The biogas samples that were obtained from the headspace of both batch and

UASB reactors, with a gas-tight syringe equipped with a pressure lock were injected into a gas chromatograph (GC-2010plusAT, SHIMADZU, Kyoto, Japan) equipped with a thermal conductivity detector (TCD) for the determination of the biogas composition as previously described from Kalamaras et al. [8]. The surface morphology of the biocarriers samples was examined using a Jeol JSM-7401F Field Emission Scanning Electron Microscope (SEM) with Gentle Beam mode. The utilization of Gentle Beam technology in this microscope aids in minimizing charging effects, enhancing resolution, improving signal-to-noise ratio, and increasing beam brightness. SEM imaging was conducted under standard conditions of 10 mA emission current and 2 kV accelerating voltage.

II. RESULT AND DISCUSSION

The methane production of the batch reactors was measured daily, and the accumulative methane production curve was formed. In Figure 1 the accumulative methane production of the batch reactors is presented. It is evident from the accumulative methane production curve that by day 15, the growth of the microbial community of the batch reactors is well into its exponential phase. According to research done by Chioti, et al.[3], the optimal time to harvest the biocarriers from the batch reactors is during the exponential phase of the microbial growth, since at that phase biocarriers that were harvested for AD experiments had the best performance in terms of methane production.

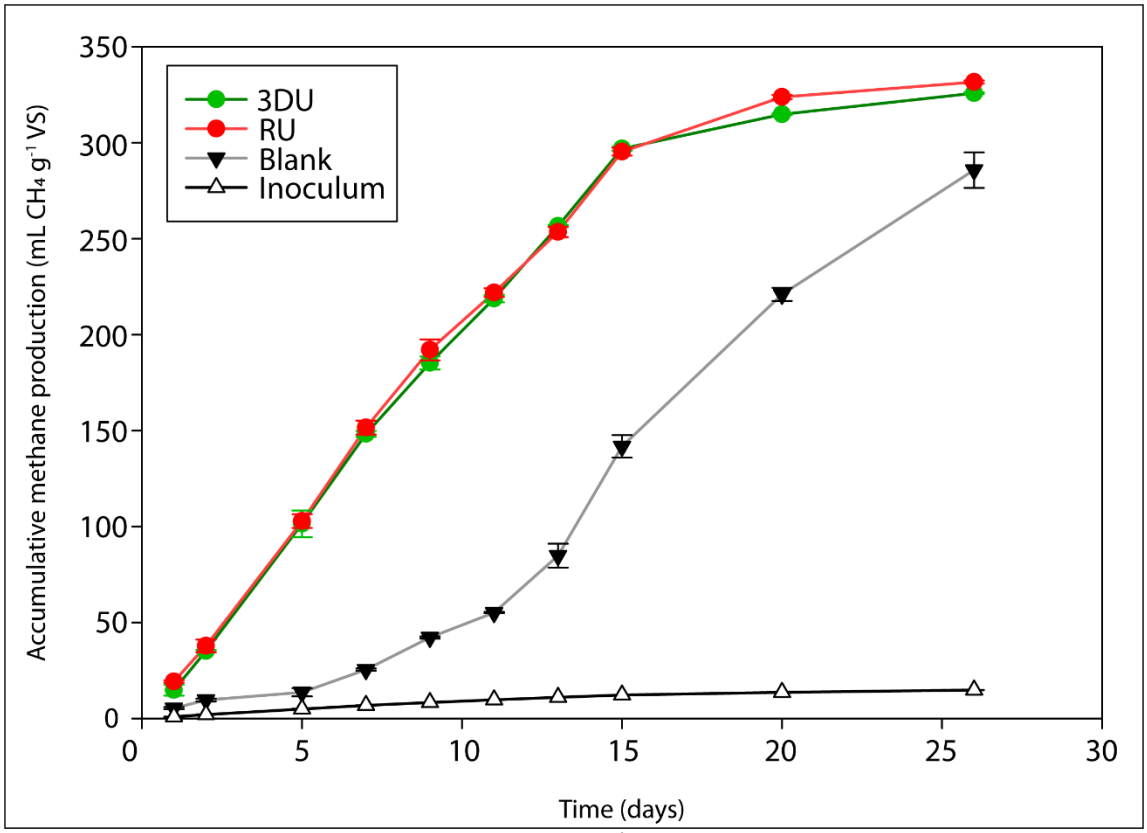

Figure 1. Accumulative methane production (mL CH_4 g^{-1} VS) from batch reactors used for the formation of biofilm on carriers.

The batch reactors containing the biocarriers (3DU, RU) clearly outperformed the Blank reactors increasing the total methane production (mL CH_4 g^{-1} VS) by 14.01% and 16.04%, respectively. Furthermore, in reactors 3DU and RU the methanogens' growth rate was higher compared to Blank reactors (285.81 ± 6.80 mL CH_4 g^{-1} VS) since it is mirrored by the rate of methane production [9]. There was not a significant difference in the total methane production of the reactors containing the 3D-printed biocarriers (3DU) and those with the K1 Rings (RU). Specifically, the 3DU and the RU reactors produced 325.86 ± 3.03 and 331.67 ± 1.81 mL CH_4 g^{-1} VS, respectively. Moreover, their accumulated methane curves of the biocarrier batch reactors followed the same general trend. Both types of biocarriers have similarly improved the methane production by AD, despite their differences in geometry and type of material. The methane production of the Inoculum reactors was 13.60 ± 0.62 mL CH_4 g^{-1} VS, an indication that its residual methane potential has been adequately reduced prior to the experimental process described above (section 1.1.2).

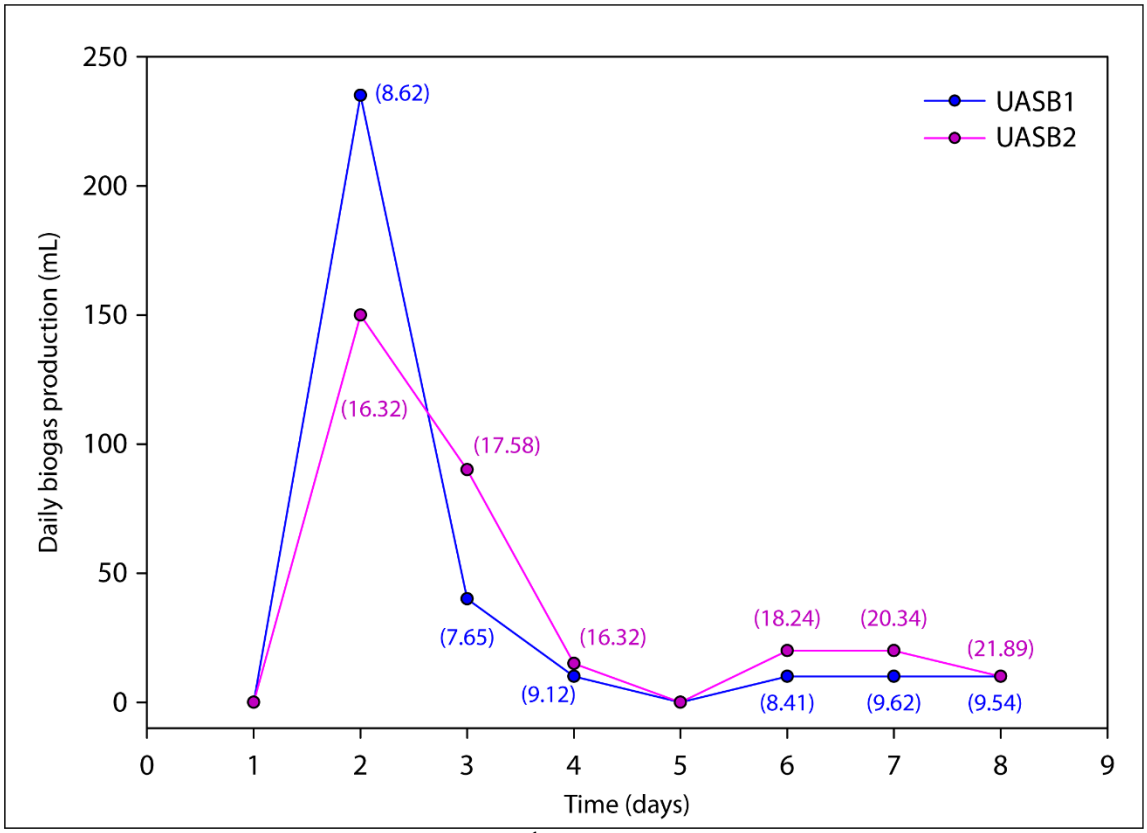

Figure 2. Daily biogas production (mL biogas d^{-1}) from UASB reactors during 1st Attempt. The number inside parentheses represent the percentage (%) of methane in biogas.

Initially, 100 mL of the two biofilm coated carriers were harvested at the exponential phase of methane production and added in each UASB reactor (UASB1, 3D-printed biocarriers and UASB2, K1 Ring biocarriers). Afterwards, both reactors were filled with 400 mL of BA medium. The operating HRT was 4 days and the OLR of the synthetic substrate was 1 g VS d^{-1} L^{-1}. The reactors were also equipped with recirculation pumps creating an up-flow velocity of 4 m s^{-1}. The biogas production for both reactors swiftly diminished over the course of 8 days, eventually stopping completely making this the 1st attempt to initiate AD in the UASB reactors. In Figure 2 the daily biogas production of the UASB reactors during the 1st attempt is presented. The VFAs concentration in both reactors increased with time, as it is shown in Table 2, a clear indication of the methanogens' reduced activity [10]. Moreover, VFAs concentration increased when biogas production simultaneously decreased and remained low for the same period. The increased VFAs concentration also caused a change in the initial pH value of 7.1, which dropped to 5.5 between 6 to 8 days from the start of AD. As AD relies on a delicate balance of microbial communities to efficiently convert organic matter into biogas, a significant increase in VFAs production without a corresponding increase in methane production can indicate an imbalance in the microbial ecosystem. Specifically, this imbalance can affect methanogens, as they can be inhibited by these intermediate products of AD [11].

After the 1st attempt, the operation of the UASB reactors was stopped and they were thoroughly cleaned and sanitized. The inability to maintain AD in the reactors, could possibly be due to the high rate of recirculation, not allowing the methanogens to establish communities on the biocarriers. Also, the large volume of BA medium used to fill the reactors has probably diluted the microbial biomass used for inoculation as it was only introduced into reactors by the attached biomass of biocarriers. Therefore, a 2nd attempt was made and the UASB reactors were filled with new 100 mL of biofilm coated carriers, 100 mL of BA medium and 300 mL of inoculum to assist in maintaining the biofilm formation on the carriers. The recirculation pumps were removed from the UASB reactors setup, and their operation started again defining the 2nd attempt. On days 1, 3, 6 and 8 (marked with red arrows in Figure 3) the reactors were manually dosed with 10 mL of D-glucose aqueous solution with a concentration of 100 g L^{-1}. On day 10, the UASB reactors were connected to a peristaltic pump and commenced automatic dosing with the synthetic substrate, operating with 4 days 1 g VS d^{-1} L^{-1} OLR. In Figure 3 the daily biogas production of the UASB reactors during the 2nd start-up attempt is presented. As it is evident from Figure 3, during the period of manual dosing the operation of the UASB reactors was probably stable. After 3 days of operation with automatic substrate dosing the biogas production of the reactors dropped drastically and although the automatic dosing was stopped it was impossible to recover the reactors' operation. Similarly, to the 1st attempt,

the VFA concentration for both reactors increased rapidly during the automatic dosing period, as presented in Table 2.

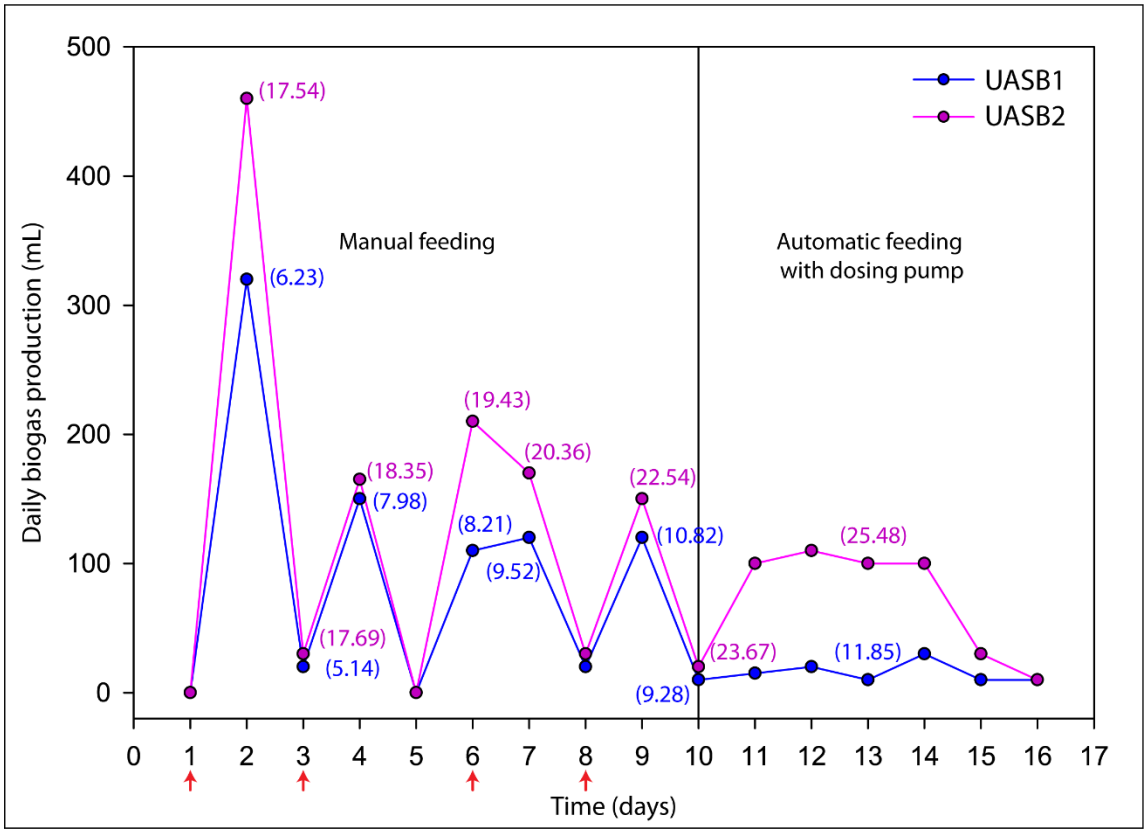

Figure 3. Daily biogas production (mL biogas d^{-1}) from UASB reactors during 2nd Attempt. The number inside parentheses represent the percentage (%) of methane in biogas.

Table 2. Total VFA (mg L^{-1}) (Mean ± SD*)

1st Attempt			2nd Attempt		
Day	UASB1	UASB2	Day	UASB1	UASB2
3	395.22 ± 12.3	370.12 ± 13.4	9	553.54 ± 17.8	108.57 ± 8.1
6	976.93 ± 9.5	1048.59 ± 25.7	13	3080.22 ± 50.6	682.51 ± 15.3
			15	1681.09 ± 22.7	90.58 ± 10.5

*SD, Standard Deviation.

Micrographs obtained by SEM analysis depict the 3d-printed biocarriers' microstructure and give a possible explanation for the fail to keep the biofilm anchored on the pore walls of the 3D-printed scaffold under the conditions of anodic flow in the bioreactor. The use of bentonite as inorganic binder between the particles of 13X zeolite, though services toward enhancing the mechanical stability of the all-ceramic biocarriers, seems to act as inhibitor of the biofilm's growth and stabilisation for two reasons. Firstly, as shown in Figure 4a the external surface of the large zeolitic crystallites (5μm) becomes very rough and this may cause difficulties to the attachment and anchoring of microorganisms. Secondly, there are many regions within the microstructure of the biocarrier where sections of the bentonite's layers protrude in the void space between the aggregated particles of 13X. As such, bentonite layers make the inter-particle space inaccessible to microorganisms. It may also be the case that they do not allow the formation of a continuous biofilm layer within the macropore structure. These hamper the stability of the biofilm since the best biofilm growing regions within a scaffold are inside their macropores.

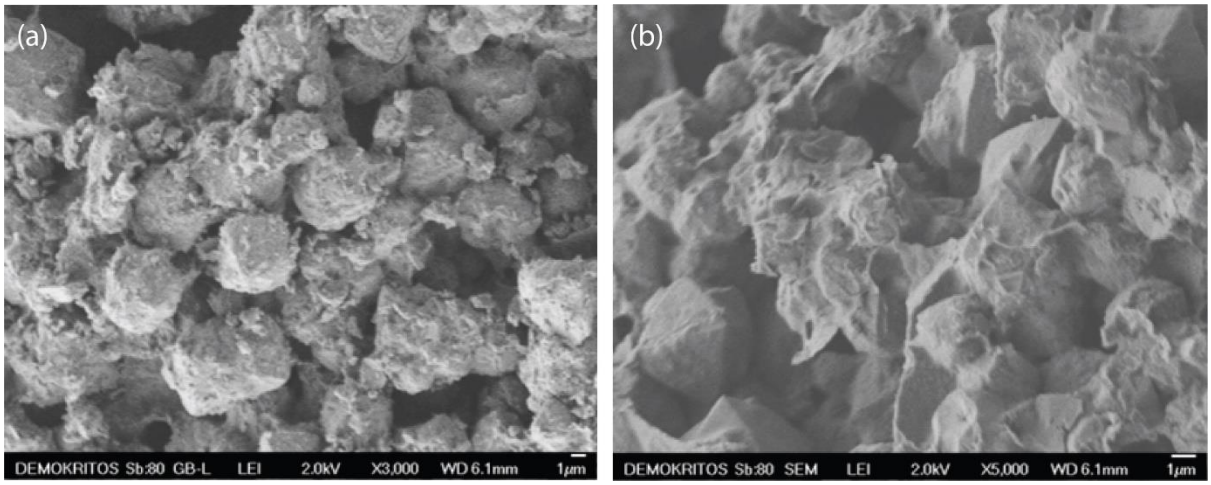

Figure 4. Micrographs of 3d-printed biocarriers obtained by SEM analysis: (a) x 3,000 and (b) x 5,000.

Several useful conclusions can be drawn from the present study, despite the UASB reactors' inability to maintain the AD process. The addition of biocarriers in the batch reactors had a positive effect on the methane production from AD, but it is important to note that the increase in methane production was similar for both types of biocarriers. In contrast, neither type of biocarrier was particularly effective at establishing and maintaining the AD Process in the UASB reactors. It is evident from these results that the physicochemical properties of the biocarriers could have a significant effect on the operation of the UASB reactors. The porosity of the biocarriers material should be sufficient in size to be available for methanogens to enter and establish communities on the biocarriers. Due to the porous size of the biocarrier material, microbial aggregates were protected by the porous structure and are more difficult to disrupt. The diameter of the methanogens ranges from 0.8-4 μm [12], so the mesoporous of the biocarriers could possibly be an important factor of their performance. Furthermore, during the 2nd Attempt, biogas analyses from UASB1 showed trace amounts of hydrogen (H_2). This indicates that the novel 3D-printed biocarriers may not favor the formation of biofilm by methanogens but by hydrogenogenic bacteria, a matter that requires further investigation.

III. CONCLUSION

The objective of this study was to develop a method for reducing the start-up period of upflow anaerobic sludge blanket (UASB) reactors. The batch reactors equipped with biocarriers demonstrated enhanced performance compared to the blank reactors, resulting in increased total methane production. However, when attempting to transfer the biocarriers from the batch reactors to the UASB reactors to expedite the start-up period, the anaerobic digestion process could not be sustained despite two attempts. It is likely that the geometrical characteristics, pore size, and material composition of the biocarriers played a role in the failure of the UASB reactors as was also supported by the SEM analysis.

REFERENCES

[1]. Chinea, L., et al., Methane enrichment of biogas using carbon capture materials. Fuel, 2023. **334**: p. 126428.
[2]. Mainardis, M., M. Buttazzoni, and D. Goi, Up-Flow Anaerobic Sludge Blanket (UASB) Technology for Energy Recovery: A Review on State-of-the-Art and Recent Technological Advances. 2020. **7**: p. 43.
[3]. Chioti, A.G., et al., Characterization of Biofilm Microbiome Formation Developed on Novel 3D-Printed Zeolite Biocarriers during Aerobic and Anaerobic Digestion Processes. Fermentation, 2022. **8**(12): p. 746.
[4]. Raj Deena, S., et al., Efficiency of various biofilm carriers and microbial interactions with substrate in moving bed-biofilm reactor for environmental wastewater treatment. Bioresource Technology, 2022. **359**: p. 127421.
[5]. Angelidaki, I. and W. Sanders, Assessment of the anaerobic biodegradability of macropollutants. Re/Views in Environmental Science & Bio/Technology, 2004. **3**(2): p. 117-129.
[6]. American Public Health, A., et al., Standard methods for the examination of water and wastewater. 21st ed ed. 2005, Washington, D.C.: APHA-AWWA-WEF.
[7]. Kalamaras, S.D., et al., The Effect of Ammonia Toxicity on Methane Production of a Full-Scale Biogas Plant—An Estimation Method. Energies, 2021. **14**(16): p. 5031.
[8]. Kalamaras, S.D., et al., Microbial adaptation to high ammonia concentrations during anaerobic digestion of manure-based feedstock: biomethanation and 16S rRNA gene sequencing. Journal of Chemical Technology & Biotechnology, 2020. **95**(7): p. 1970-1979.
[9]. Christou, M.L., et al., Effects of organic loading rate and hydraulic retention time on bioaugmentation performance to tackle ammonia inhibition in anaerobic digestion. Bioresource Technology, 2021. **334**: p. 125246.
[10]. Christou, M.L., et al., Ammonia-induced inhibition of manure-based continuous biomethanation process under different organic loading rates and associated microbial community dynamics. Bioresource Technology, 2021. **320**: p. 124323.
[11]. Wang, Y., et al., Effects of volatile fatty acid concentrations on methane yield and methanogenic bacteria. Biomass and Bioenergy, 2009. **33**(5): p. 848-853.
[12]. Wagner, D., Methanosarcina, in Bergey's Manual of Systematics of Archaea and Bacteria. 2020. p. 1-23.